Titin-based stiffening of muscle fibers in Ehlers-Danlos Syndrome

Coen A. C. Ottenheijm, Nicol C. Voermans, Bryan D. Hudson, Thomas Irving, Ger J. M. Stienen, Baziel G. van Engelen and Henk Granzier

J Appl Physiol 112:1157-1165, 2012. First published 5 January 2012;
doi:10.1152/japplphysiol.01166.2011

Journal of Applied Physiology publishes original papers that deal with diverse areas of research in applied physiology, especially those papers emphasizing adaptive and integrative mechanisms. It is published 12 times a year (monthly) by the American Physiological Society, 9650 Rockville Pike, Bethesda MD 20814-3991. ISSN: 0363-6143, ESSN: 1522-1563. Visit our website at http://www.the-aps.org/.

J Appl Physiol 112: 1157–1165, 2012.
First published January 5, 2012; doi:10.1152/japplphysiol.01166.2011.

Titin-based stiffening of muscle fibers in Ehlers-Danlos Syndrome

Coen A. C. Ottenheijm,[1,3] Nicol C. Voermans,[2] Bryan D. Hudson,[3] Thomas Irving,[4] Ger J. M. Stienen,[1] Baziel G. van Engelen,[2] and Henk Granzier[3]

[1]*Laboratory for Physiology, Institute for Cardiovascular Research, VU University Medical Center, Amsterdam;* [2]*Department of Neurology, Radboud University Nijmegen Medical Center, Nijmegen, The Netherlands;* [3]*Department of Physiology, University of Arizona, Tucson, Arizona; and* [4]*Department of Biological, Chemical and Physical Sciences, Illinois Institute of Technology, Chicago, Illinois*

Submitted 19 September 2011; accepted in final form 3 January 2012

Ottenheijm CAC, Voermans NC, Hudson BD, Irving T, Stienen GJM, van Engelen BG, Granzier H. Titin-based stiffening of muscle fibers in Ehlers-Danlos Syndrome. *J Appl Physiol* 112: 1157–1165, 2012. First published January 5, 2012; doi:10.1152/japplphysiol.01166.2011.— *Objective*: tenascin-X (TNX) is an extracellular matrix glycoprotein whose absence leads to Ehlers-Danlos Syndrome (EDS). TNX-deficient EDS patients present with joint hypermobility and muscle weakness attributable to increased compliance of the extracellular matrix. We hypothesized that in response to the increased compliance of the extracellular matrix in TNX-deficient EDS patients, intracellular adaptations take place in the elastic properties of the giant muscle protein titin. *Methods*: we performed extensive single muscle fiber mechanical studies to determine active and passive properties in TNX-deficient EDS patients. Gel-electrophoresis, Western blotting, and microarray studies were used to evaluate titin expression and phosphorylation. X-ray diffraction was used to measure myofilament lattice spacing. *Results*: passive tension of muscle fibers from TNX-deficient EDS patients was markedly increased. Myofilament extraction experiments indicated that the increased passive tension is attributable to changes in the properties of the sarcomeric protein titin. Transcript and protein data indicated no changes in titin isoform expression. Instead, differences in posttranslational modifications within titin's elastic region were found. In patients, active tension was not different at maximal activation level, but at submaximal activation level it was augmented attributable to increased calcium sensitivity. This increased calcium sensitivity might be attributable to stiffer titin molecules. *Conclusion*: in response to the increased compliance of the extracellular matrix in muscle of TNX-deficient EDS patients, a marked intracellular stiffening occurs of the giant protein titin. The stiffening of titin partly compensates for the muscle weakness in these patients by augmenting submaximal active tension generation.

passive stiffness; muscle weakness

TENASCIN-X (TNX) is an extracellular matrix glycoprotein whose absence leads to a recessive form of Ehlers-Danlos Syndrome (EDS), a group of related heritable connective tissue disorders with joint hypermobility, hyperextensible skin, tissue fragility, and easy bruising (3, 4, 32). Recently, we have shown that TNX-deficient EDS patients present with mild to moderate neuromuscular involvement (38). Myalgia and easy fatigability are reported frequently, and mild-to-moderate muscle weakness is common. Ultrastructural analysis showed preserved sarcomeric structure and reduction of collagen fibril density and length in the endomysium (38). Quantitative muscle function tests in TNX-deficient EDS patients (36), as well as in TNX-knockout mice (17), revealed increased compliance of the connective tissue within the muscle-tendon complex and between adjacent muscles. As a result, the connective tissue in TNX-deficient muscle is less capable of transmitting forces within and between adjacent muscles, and muscles probably act more independently and less efficiently. Thus the muscle weakness in TNX-deficient EDS patients is likely caused by the increased compliance of the connective tissue surrounding the muscle fibers.

Here we investigated whether the *extra*cellular alterations of connective tissue result in *intra*cellular changes in muscle fiber function in TNX-deficient EDS patients. It is now well recognized that the extracellular matrix is an extremely dynamic complex of molecules that interacts through trans-sarcolemmal structures with cytoskeletal elements that are part of the contractile units of muscles, the sarcomeres. This is important to maintain skeletal muscle integrity and to transmit forces (19). Thus changes in the extracellular matrix might affect sarcomeric properties and alter muscle fiber function. Such interplay between extracellular matrix proteins and intracellular structures has been observed in other disorders. For instance, recent studies revealed that increased stiffness of the extracellular matrix in heart muscle, attributable to elevated collagen expression, was followed by expression of more compliant titin molecules to compensate for the increased ventricular stiffness (41).

Titin is a giant sarcomeric protein (3–4 MDa) that spans the half-sarcomeric distance from the Z-disk to the M-band, thus forming the third sarcomeric filament, in addition to the thick (mostly myosin) and thin (mostly actin) filaments (24, 29) (for schematic see Fig. 3*C*). In the sarcomere's I-band region, titin is extensible and functions as a molecular spring that develops passive tension upon stretch. In skeletal muscle, an important source of titin's elasticity is the segment rich in proline, glutamate, valine, and lysine (PEVK) residues. These elastic properties of titin are crucial in maintaining the structural integrity of the sarcomere and are essential for optimal muscle fiber function (22).

In the present study we hypothesized that in response to the increased compliance of the extracellular matrix, muscle fibers in TNX-deficient EDS patients stiffen due to changes in the elastic properties of titin. To test this hypothesis, we performed extensive studies to determine the active and passive properties of quadriceps femoris muscle fibers from TNX-deficient EDS patients. In line with our hypothesis, we found that in TNX-deficient EDS patients sarcomeric stiffness is markedly increased because of changes in titin's elastic properties. We propose that these changes constitute an intracellular mechanism to compensate for the muscle weakness caused by the

Address for reprint requests and other correspondence: C. Ottenheijm, VU Univ. Medical Center, Dept. of Physiology, Amsterdam, The Netherlands (e-mail: c.ottenheijm@vumc.nl).

more compliant extracellular matrix in TNX-deficient EDS patients.

MATERIALS AND METHODS

Muscle Biopsies from EDS Patients

Quadriceps femoris biopsies were collected from four patients with EDS attributable to tenascin-X deficiency (age range 20–38 yr; 2 men, 2 women; for additional patient characteristics see Table 1 and Ref. 38) and from four unaffected controls (age range 20–30 yr; 3 men, 1 woman) following written informed consent supervised by the Radboud University Nijmegen Medical Center and stored frozen and unfixed at −80°C until use.

Muscle Mechanics

Muscle mechanics were performed as described previously (26, 28, 30). In brief, small strips dissected from muscle biopsies were thawed in 50% glycerol/relaxing solution (25, 26, 28, 30) and skinned overnight. The skinning procedure renders the membranous structures in the muscle fibers permeable, which enables activation of the myofilaments with exogenous Ca^{2+}. Preparations were washed thoroughly with relaxing solution (26) and stored in 50% glycerol/relaxing solution at −20°C for up to ~8 wk. Single muscle fibers were dissected from the skinned strips and were mounted between a displacement generator and a force transducer element (AE 801, SensoNor, Norway) using aluminum T-clips. For all contractile parameters 6–10 single fibers were analyzed per subject. Sarcomere length (SL) was set using an online He-Ne laser diffraction system (12). Mechanical experiments on contracting muscle were carried out at an SL of ~2.5 μm. Fiber width and diameter were measured at three points along the fiber, and the cross-sectional area (CSA) was determined assuming an elliptical cross section. Three different bathing solutions were used during the experimental protocols: a relaxing solution, a pre-activating solution with low EGTA concentration, and an activating solution (pCa 4.5). The composition of these solutions has been described previously (33). The preparation was activated at pCa 4.5 to obtain maximal Ca^{2+}-activated force. Maximal stress was determined by dividing the force generated at pCa 4.5 by CSA.

Determination of passive tension. For determination of passive tension (passive force divided by single fiber CSA) single muscle fibers were set at slack length in relaxing solution. Then passive force was recorded while SL was increased to ~3.0 μm (velocity, 0.1 muscle length/s), followed by a release back to the slack length. Subsequently, thick and thin filaments were extracted by immersing the preparation in relaxing solution containing 0.6 M KCl (35 min at 20°C) followed by relaxing solution containing 1.0 M KI (35 min at 20°C). Following the extraction procedure, the muscle fibers were stretched again at the same velocity and the passive force remaining after KCl/KI treatment was assumed to be non-titin based and titin-based passive force was determined as total passive force minus non-titin-based passive force (7, 8, 10, 25, 27).

Simultaneous active force-ATPase measurement. We used the system described by Stienen et al. (33). To measure the ATPase activity, a near ultraviolet (UV) light was projected through the window of the bath (30 μl volume and temperature controlled at 20°C) and detected at 340 nm. The maximum activation buffer (pCa 4.5) contained 10 mM phosphoenol pyruvate, with 4 mg/ml pyruvate kinase (500 U/mg), 0.24 mg/ml lactate dehydrogenase (870 U/mg), and 20 μM diadenosine-5′ pentaphosphate (A_2P_5). For efficient mixing, the solution in the bath was continuously stirred by means of motor-driven vibration of a membrane positioned at the base of the bath. ATPase activity of the skinned fiber was measured as follows: ATP regeneration from ADP is coupled to the breakdown of phosphoenol pyruvate to pyruvate and ATP catalyzed by pyruvate kinase, which is linked to the synthesis of lactate catalyzed by lactate dehydrogenase. The breakdown of NADH, which is proportional to the amount of ATP consumed, is measured online by UV absorbance at 340 nm. The ratio of light intensity at 340 nm (sensitive to NADH concentration), and the light intensity at 400 nm (reference signal) is obtained by means of an analog divider. After each recording, the UV absorbance signal of NADH was calibrated by multiple rapid injections of 0.25 nmol of ADP (0.025 μl of 10 mM ADP) into the bathing solution, with a stepper motor-controlled injector. The slope of the [ATP] vs. time trace during steady-state tension development of a Ca^{2+}-induced contraction (see Fig. 2*C*) was determined from a linear fit and the value divided by the fiber volume (in mm^3) to determine the fiber's ATPase rate. ATPase rates were corrected for the basal ATPase measured in relaxing solution. The ATPase rate was divided by tension (force/CSA) to determine the tension cost.

Force-pCa relations. To determine the force-pCa relation (pCa = −log of molar free Ca^{2+} concentration), skinned muscle fibers were sequentially bathed in solutions with pCa values ranging from 4.5 to 9.0 and the steady-state force was measured. Measured force values were normalized to the maximal force obtained at pCa 4.5. The obtained force-pCa data were fit to the Hill equation, providing pCa_{50} (pCa giving 50% maximal active tension) and the Hill coefficient, n_H, an index of myofilament cooperativity. Note that type 2A muscle fibers from the TNX-deficient patients had too much force rundown (>10%) during the protocol and were therefore excluded from analysis.

X-Ray Diffraction Studies

Small-angle X-ray diffraction experiments were performed at the BioCAT beamline 18ID (Argonne National Laboratory, Argonne, IL).

Table 1. *Patient characteristics*

	Patient 1	*Patient 2*	*Patient 3*	*Patient 4*
Mutation analysis of *TNXB*	n.p.	n.p.	n.p.	Homozygous for 30 kB deletion.
TNX in serum	0	0	0	0
Sex and age (yr) at time of clinical investigations	Female, 22	Male, 20	Male, 27	Female, 38
Beighton score (generalized joint hypermobility if ≥5)	8	9	9	8
Muscle strength (MRC) sum score 0–140; sum of 28 muscles tested (average MRC)	127 (4.5)	130 (4.6)	140 (5)	115 (4.1)
Quadriceps muscle biopsy, histology	Type I > type II fibers; overall normal	Mild increase type IIX fibers; overall normal	Type II > type I fibers; overall normal	Type II > type I fibers; overall normal
Atrophy of quadriceps muscle on ultrasound (Z >2.0)	no	no	no	no

TNX, tenascin-X; MRC, Medical Research Council; n.p., not performed. Note that *TNXB* mutation analysis was not performed in all patients, because it is a large gene and sequention analysis was time-consuming/expensive, especially at the time these patients were diagnosed. Instead, this type of Ehlers-Danlos Syndrome (EDS) has been diagnosed by the absence of TNX in serum, suggesting a homozygous or compound heterozygous *TNXB* mutation.

Single muscle fibers were mounted on a custom X-ray diffraction/muscle mechanics setup designed to fit into the X-ray diffraction instrument. Muscle fibers were attached between a high-speed motor (Cambridge model 308B, ~1 ms 90% step response) and a force transducer (KG4 SI Heidelberg, 0.1–10 mN working range). Sarcomere length was determined using the first-order diffraction band from a He-Ne laser captured on a linear CCD with a 2 kHz refresh rate (model PLIN-2605–2 Dexela, London, UK). Passive tension, sarcomere length, and lattice spacing were simultaneously measured. The X-ray exposure times were ~0.5 s, and the X-ray diffraction patterns were collected with the use of a CCD-based area detector. The lattice spacing and sarcomere length were measured in relaxed preparations as described previously (22). Separation of the 1,0 equatorial reflections measured from the diffraction pattern were converted to d1,0 lattice spacing via Bragg's law, which can be converted to inter-thick-filament spacing by multiplying d1,0 by $2/\sqrt{3}$.

Microarray Studies

Microarray studies were performed as described previously (27). In brief, muscle tissues from all patients and control subjects were collected in RNAlater from Ambion (Austin, TX). The tissue was homogenized using a Pro200 homogenizer from *PRO* Scientific RNA was isolated using the Qiagen RNeasy Fibrous Tissue Mini Kit. RNA was amplified using the SenseAmp kit from Genisphere and Superscript III reverse transcriptase enzyme from Invitrogen. Reverse transcription and dye coupling (Alexa Fluor 555 and Alexa Fluor 647 were used) was done using Invitrogen's superscript plus indirect cDNA labeling module. Half of each sample was incorporated with Alexa Fluor 555 and the other with Alexa Fluor 647. We used a home-made titin exon microarray that consisted of 50mer oligonucleotides representing each of 363 human titin exons (selected for GC content 45–55%; Tm ~ 70°C and minimal tendency for hairpin structures and dimerization). Exons were spotted in triplicate on Corning Ultra GAPS glass slides. Slides were then baked at 90°C for 90 min and stored in a nonelectric desiccator. Hybridization (Ambion: Slide-Hyb buffer #1) occurred for 16 h at 42°C, after which slides were scanned at 595 nm and 685 nm with an Array WoRx scanner. Spot finding was done with SoftWoRx Tracker. Spot files were analyzed using CARMA, which provides a quantitative and statistical characterization of each measured exon. Normalization between the two channels of each array was achieved by performing a locally weighted regression (lowess) transformation that adjusts for intensity and location dependent effects [for details, see Greer et al. (13)].

Gel-Electrophoresis

For titin mobility studies, SDS-agarose electrophoresis was performed as previously described (27, 40). In short, muscle samples were pulverized to a fine powder and then rapidly solubilized and analyzed by vertical SDS-agarose electrophoresis. Because there is a slight gel-to-gel variation in migration patterns titin mobility was quantified by mixing samples of interest with chicken pectoralis, providing two constant mobility markers in the form of chicken pectoralis T1 (full-length titin) and chicken pectoralis nebulin. The distance on the gel between the chicken pectoralis nebulin and T1 from the sample of interest was divided by the distance between chicken pectoralis nebulin and chicken pectoralis T1 to yield a measure of relative titin size. The obtained values for relative titin size were insensitive to gel-to-gel variation (as determined by using identical samples on gels that were electrophoresed for greatly differing times). For determination of the total titin:myosin heavy chain (MHC) ratio the integrated optical density of total titin and MHC were determined as a function of the volume of solubilized protein sample that was loaded (a range of volumes was loaded on each gel). The slope of the linear range of the relation between integrated optical density and loaded volume was obtained for each protein.

Western Blotting

For Western blotting with the anti-titin antibody 9D10, samples were run on 1% agarose gels and transferred to PVDF membrane using a semi-dry transfer unit (Bio-Rad, Hercules, CA). The blots were stained with PonceauS to visualize total transferred protein. The blots were then probed with 9D10 antibody [which is specific for the PEVK region of titin (34)]. 9D10 labeling was normalized to total titin obtained from the PonceauS stained blot. Secondary antibodies conjugated with fluorescent dyes with infrared excitation spectra were used for detection. One-color IR Western blots were scanned (Odyssey Infrared Imaging System, Li-Cor Biosciences), and the images were analyzed with One-D scan EX.

For Western blotting with phospho-specific antibodies, samples were run on 1% agarose gels and transferred to PVDF membrane as described above. Blots were stained with PonceauS to visualize total transferred protein. The blots were then probed with rabbit polyclonal antibodies against titin's pS26 (GenScript, 1:100) and pS170 (Genscript, 1:100). To normalize for loading differences, phosphorylated titin labeling was normalized to total protein, determined from the PonceauS-stained membrane. Secondary antibodies conjugated with fluorescent dyes with infrared excitation spectra were used for detection as described above.

Statistical Analysis

The data are presented as means ± SE. Statistical analyses were performed by *t*-test; $P < 0.05$ was considered statistically significant.

RESULTS

Increased Passive Stiffness of Sarcomeres in Fibers from TNX-Deficient Patients

To study passive muscle fiber stiffness we determined the development of passive tension over a range of sarcomere lengths in relaxed skinned muscle fibers from TNX-deficient EDS patients and from control subjects. Passive force was normalized to fiber cross-sectional area to obtain passive tension. Because it has been shown that the passive tension of type 1 and type 2A fibers does not differ (31), data from type 1 and type 2A fibers were pooled [note that no type 2X fibers were detected, which is consistent with the low abundance of type 2X fibers in human m. quadriceps (28)]. We found that the passive tension was significantly increased at all sarcomere lengths in muscle fibers from patients with TNX deficiency (Fig. 1*A*, *left*), ranging from >300% of control values at short sarcomere lengths to ~200% of control values at the longer sarcomere length range (2.6–3.0 μm, Fig. 1*A*, *right*).

To verify that the increased passive tension in TNX-deficient muscle fibers is titin based and not attributable to intermediate filaments or cross-bridge cycling at low calcium concentrations, we performed two additional sets of experiments. First, we studied the effect of depolymerizing the thin and thick filaments (with high concentrations of KI and KCl, respectively) on passive stiffness. Depolymerizing the thin and thick filaments leaves titin unanchored and, therefore, abolishes titin-based passive tension. As shown in Fig. 1*B*, depolymerization of thin and thick filaments completely abolished passive tension generation in both TNX-deficient and control fibers. Second, to rule out that the increased passive tension in TNX-deficient fibers is caused by cross-bridge cycling at low calcium concentrations, fibers were treated with gelsolin to cleave the thin filaments. Cleavage of the thin filaments makes tension generation attributable to actomyosin interaction im-

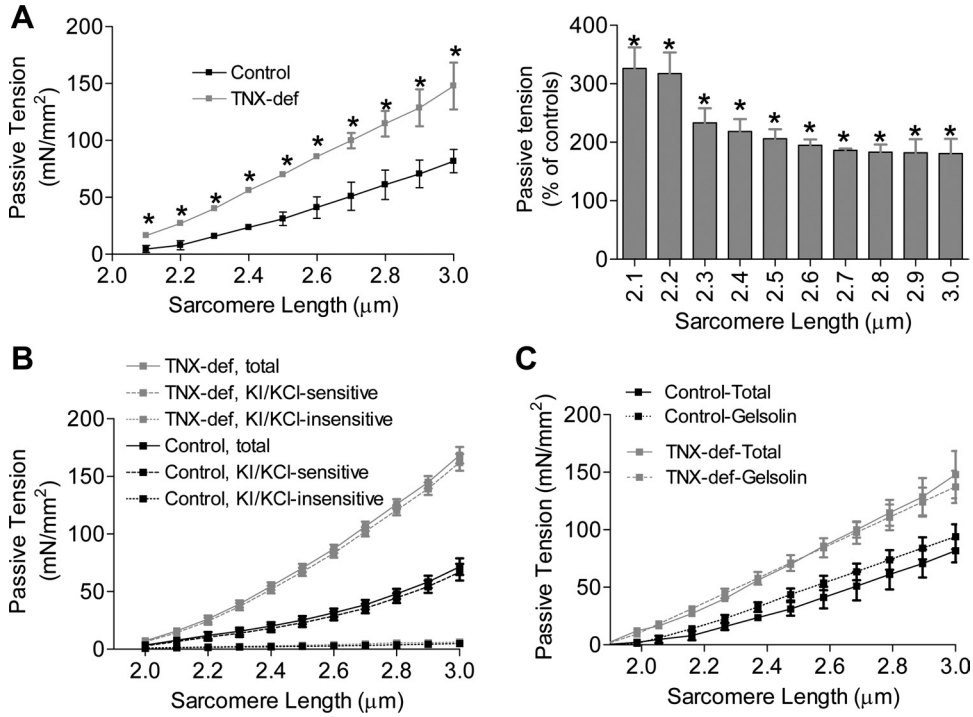

Fig. 1. Passive tension of muscle fibers from tenascin-X (TNX)-deficient Ehlers-Danlos Syndrome (EDS) patients and controls. *A*: total passive tension as a function of sarcomere length is significantly elevated in patient fibers. *B*: passive tension before and after extraction of thick and thin filaments with KCL/KI treatment (for details see MATERIALS AND METHODS). Note that the passive tension after extraction is negligible in fibers from both patient and control fibers, suggesting that the total passive tension before extraction was myofilament based. *C*: passive tension after gelsolin treatment, which extracts exclusively the thin filament and abolishes cross-bridge interaction. Note that gelsolin treatment has no significant effect on passive tension in both patients and control fibers, suggesting that residual cross-bridge cycling does not contribute to passive tension. Values shown are means ± SE. $*P < 0.05$ compared with controls.

possible but does not affect titin. As shown in Fig. 1*C*, gelsolin treatment did not significantly affect passive tension generation, indicating that the increased passive tension in TNX-deficient muscle fibers is not caused by cross-bridge interaction. Together, these results strongly suggest that the increased passive stiffness of muscle fibers from patients with TNX deficiency is titin based.

To study whether the changes in passive tension were accompanied by changes in active tension, we studied the maximum force generating capacity of single muscle fibers from patients with TNX deficiency and from control subjects. We exposed skinned muscle fibers to a saturating calcium concentration and measured the force response; Fig. 2*A* shows a typical force response from a control and patient muscle fiber. We found that the maximum active tension of both type 1 and 2A fibers was not significantly different between muscle fibers from TNX-deficient patients and those from control subjects (Fig. 2*B*). Thus these findings indicate that the maxi-

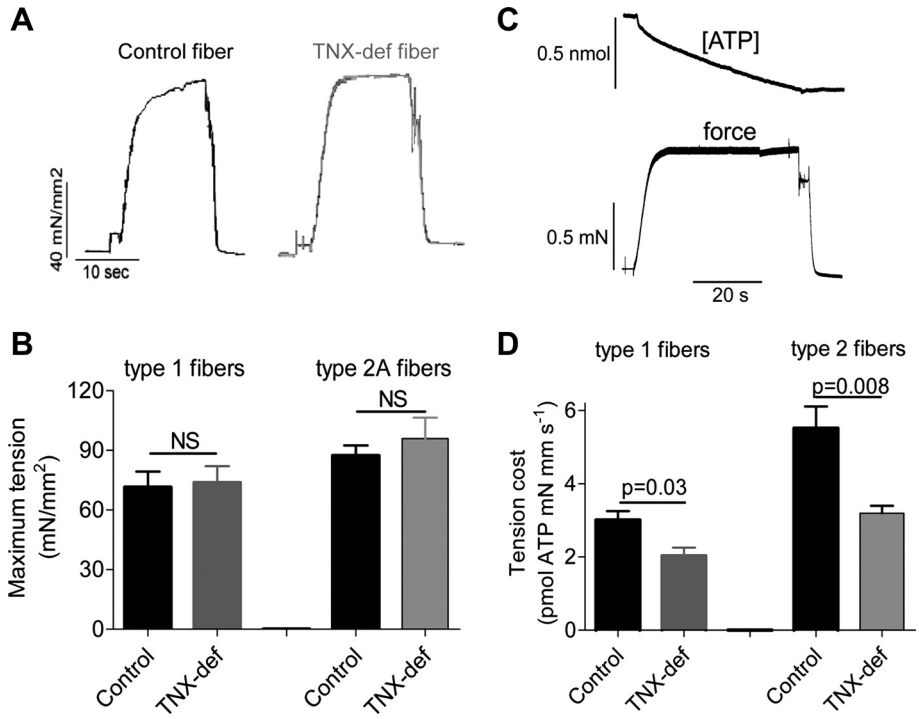

Fig. 2. *A*: typical force response to saturating Ca^{2+} levels of a control fiber and a fiber from an EDS patient with TNX deficiency. Note the comparable maximum force levels. *B*: maximum stress (force normalized to fiber cross-sectional area) is the same in fibers from EDS patients with TNX deficiency and control subjects in both type 1 and type 2A fibers. Values shown are the means ± SE. *C*: tension cost of patient and control fibers; example of a maximally activated patient fiber (pCa 4.5) with developed force at the *bottom* and [ATP] at the *top*. Slope of the [ATP] vs. time trace was divided by fiber volume (in mm^3) to determine the ATP consumption rate. *D*: ATP consumption rate was normalized to tension to determine the tension cost. The tension cost is significantly lower in fibers from EDS patients. Values shown are means ± SE.

mum force generating capacity of sarcomeres from patients with TNX deficiency is preserved.

The force generating capacity of skinned muscle fibers depends on the kinetics of cross-bridge cycling to determine the proportion of cross bridges in the force generating state. The kinetics of cross-bridge attachment and detachment can be altered in a way that does not necessarily affect net force production but does affect the rate of energy (ATP) conversion. Therefore, to study whether the kinetics of cross-bridge cycling are different between patients and controls, we determined the energetic cost of active tension in single muscle fibers. This tension cost was determined by measurement of the breakdown of NADH simultaneous with force during contraction, with NADH levels enzymatically coupled to ATP utilization (see MATERIALS AND METHODS). An example of a maximally activated patient's muscle fiber with [NADH] falling linearly during the tension plateau is shown in Fig. 2*C*. The slope of the [NADH] vs. time curve was normalized by the fiber volume to obtain ATP consumption rates that can be compared for differently sized muscle fibers. By normalizing ATP consumption rates to the tension generated and fiber volume, the tension cost can be determined. As shown in Fig. 2*D*, the tension cost was significantly lower in both type 1 and 2A muscle fibers from patients compared with those from control fibers. Thus the tension cost data suggest that cross-bridge cycling kinetics are significantly altered in muscle fibers from patients with TNX deficiency.

Titin Expression and Phosphorylation in Muscle Fibers from TNX-Deficient Patients

To explore potential molecular mechanisms underlying the markedly increased titin-based passive tension in muscle fibers from TNX-deficient muscle fibers we used a multi-disciplinary approach. Titin *content* in muscle fibers was determined using SDS-agarose gel-electrophoresis. Figure 3*A* shows a typical gel result. As shown in Fig. 3*B*, titin content, normalized to myosin have chain (MHC) content, was not different between muscle fibers from TNX-deficient patients and controls.

As titin *size* is an important determinant of passive stiffness, we next quantified relative titin size by co-electrophoresing samples of interest with chicken pectoralis, providing two constant mobility markers in the form of chicken pectoralis titin [M_r 3.0 MDa (9)] and chicken pectoralis nebulin. We determined the distance between the titin bands of the sample of interest and chicken pectoralis nebulin and divided that by the distance of chicken pectoralis titin and nebulin (all determined within the same lane on the gel). The ratio so obtained reflects relative titin size and is insensitive to gel-to-gel variation (as determined by using identical samples on gels that were electrophoresed for greatly differing times). As shown in Fig. 3*B*, *right*, relative titin size was not different between TNX-deficient patients and control subjects.

To study whether titin exon *composition* is altered in TNX-deficient muscle, we used a home-made titin exon microarray that represents all of the 363 human titin exons. Figure 3*C* shows the expression of these 363 titin exons in muscle fibers from TNX-deficient patients relative to that in controls. No significant up- or downregulation was observed in titin exon expression in muscle fibers from TNX-deficient patients. To test for altered expression of titin's extensible PEVK domain at the protein level, we used the anti-titin antibody 9D10 [previous work revealed that 9D10 exclusively labels the PEVK segment from close to its NH_2 terminal end to its COOH terminal (34, 39)]. Consistent with our transcript data, Western blotting studies with 9D10 revealed that relative to total titin (obtained from the PonceauS stained blot) expression of PEVK domains is not different between TNX-deficient and controls muscle (Fig. 3*D*). Thus these results indicate that the increased passive stiffness of muscle fibers from TNX-deficient EDS

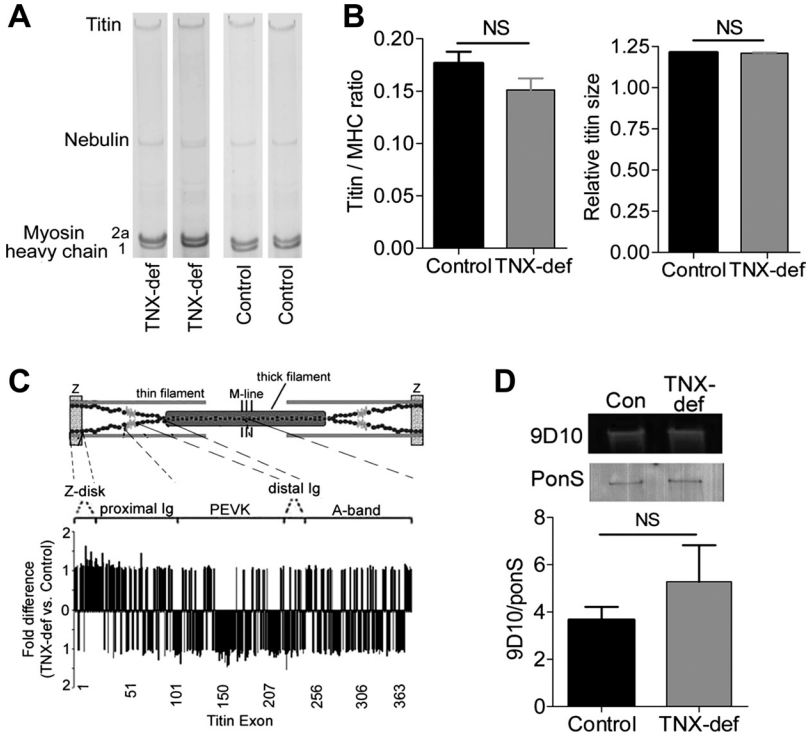

Fig. 3. *A*: SDS-agarose gel electrophoresis of quadriceps homogenates from EDS patients with TNX deficiency and controls. *B*: titin/myosin heavy chain (MHC) ratio (*left*) and titin isoform size (*right*) are not different between patients and controls (values obtained by coelectrophoresing the samples of interest with chicken pectoralis, see MATERIALS AND METHODS for details). *C*: *top*, diagram of the sarcomere; *bottom*, titin exon composition in muscle from TNX-deficient EDS patients vs. that in control muscle. Titin exon composition is not different between patient and control muscle. *D*: Western blotting studies with the proline, glutamate, valine, and lysine (PEVK)-specific anti-titin antibody 9D10. *Top*: typical Western blot result with 9D10 antibody and PonceauS (PonS) staining of total titin. *Bottom*: quantitative analysis of 9D10 staining (normalized to protein levels obtained from the PonceauS membrane) in patients and controls. Values shown are means ± SE.

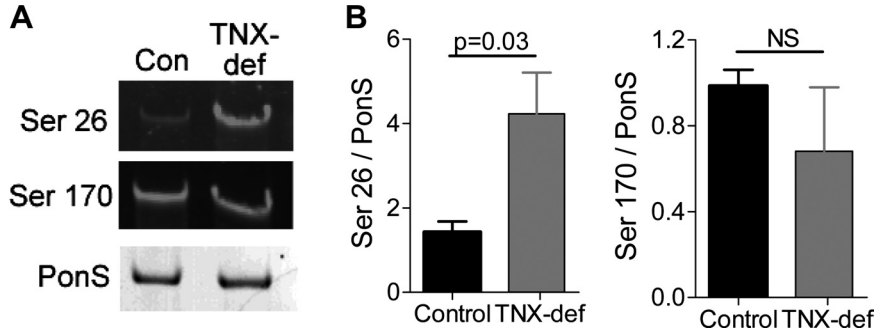

Fig. 4. Novel phospho-specific antibodies to titin's PCKα phosphorylation targeting PEVK sites, S26 and S170, were evaluated in all 4 patient and all 4 control samples. *A*: representative Western blot showing labeling of the phospho-sites and PonceauS (PonS) staining of total titin. *B*: analysis shows (*left*) hyperphosphorylation of PEVK's S26 and (*right*) no significant change in phosphorylation of S170 in patient samples. Values are means ± SE.

patients is not attributable to changes in titin content, isoform size, or exon composition.

Finally, we studied phosphorylation of titin at S11878 and S12022 (S26 and S170 in the PEVK region of N2B cardiac titin). These studies were motivated by recent evidence that suggests that S26 and S170 in cardiac titin are targets for phosphorylation by protein kinase C-α and that phosphorylation of S26 induces a large increase in passive stiffness (1, 14). Western blotting studies with phospho-specific antibodies (pS26 and pS170) revealed an approximately threefold increase of S26 phosphorylation in muscle from TNX-deficient patients compared with controls (Fig. 4). Phosphorylation of S170 was not significantly different between both groups. Thus phosphorylation of S26 in the PEVK region of titin is significantly increased in patients with TNX deficiency.

Reduced Myofilament Lattice Spacing in Muscle Fibers from TNX-Deficient Patients

Several recent lines of evidence indicate that the lateral separation of thick and thin filaments within the skeletal muscle and cardiac sarcomere (i.e., myofilament lattice spacing) is regulated by titin as a lattice stabilizer via its passive force (5, 7, 18), with stiffer titin molecules reducing myofilament lattice spacing more as muscle lengthens. Myofilament lattice spacing is important as it has been suggested to determine force generation at submaximal calcium concentrations (5, 7, 20). To explore whether myofilament lattice spacing is reduced in muscle fibers from patients with TNX deficiency, we measured myofilament lattice spacing using small angle X-ray diffraction. Figure 5*A* shows a typical equatorial X-ray pattern and 1,0 reflection from a muscle fiber from a TNX-deficient patient [note that the distance between both 1,0 reflections is used to calculate myofilament lattice spacing ($d_{1,0}$), with decreased distance indicating reduced lattice spacing]. Figure 5*B* shows that $d_{1,0}$ decreases with increasing sarcomere length, and that this relation is shifted downward in muscle fibers from patients with TNX deficiency compared with control subjects. Thus, at a given sarcomere length, the distance between thin and thick filaments is reduced in muscle fibers from TNX-deficient patients. It should be noted that upon skinning of muscle fibers lattice spacing increases. Therefore, the lattice spacings reported here overestimate those found in intact muscle fibers. However, as it is unlikely that skinning affected lattice spacing differentially in TNX-deficient vs. control fibers, the observed differences in lattice spacing between both groups are likely to be retained in intact muscle.

Elevated Ca^{2+} Sensitivity of Force Generation in Patients with TNX Deficiency

Changes in myofilament lattice spacing affect the Ca^{2+}-sensitivity of active force, an important determinant of muscle function. Therefore, we next measured the active force at a range of calcium levels and expressed force relative to the maximal force. An example of active force development of a single muscle fiber in response to incremental calcium is shown in Fig. 5*C*. Interestingly, the obtained force-pCa relations were shifted to the left in muscle fibers from TNX-

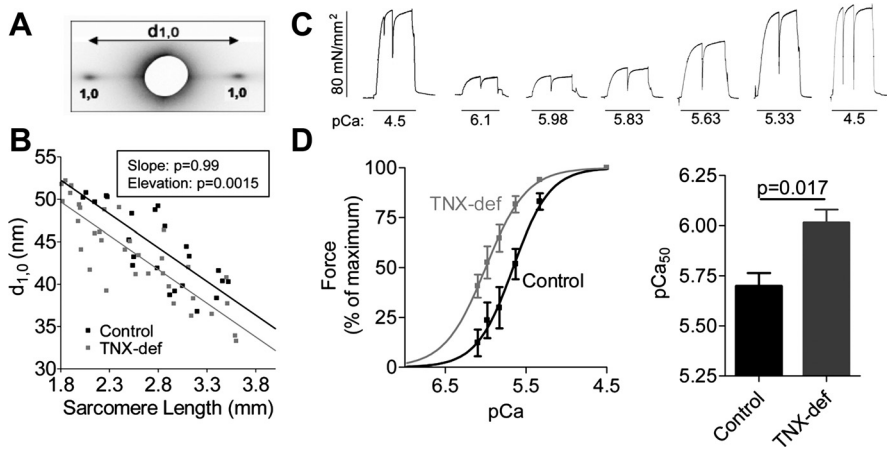

Fig. 5. *A*: X-ray diffraction studies on single muscle fibers from EDS patients with TNX deficiency and control fibers. Typical X-ray diffraction pattern showing the equatorial (i.e., perpendicular to the fiber axis) 1,0 reflections from which lattice spacing ($d_{1,0}$) is derived. *B*: myofilament lattice spacing decreases with increasing sarcomere length; note that this relation is shifted down in muscle fibers from the 4 patients compared with the 4 control subjects. *C*: force-Ca^{2+} characteristics of muscle fibers from EDS patients with TNX -deficiency and from control muscle fibers. Chart recording shows a typical force response to incremental Ca^{2+} concentrations in a patient's fiber preparation. *D*: *left*, the relative force generated in response to incubation with incremental increase of [Ca^{2+}]; note the leftward shift of the force-Ca^{2+} relationship in patients' vs. control muscle fibers. *Right*: the Ca^{2+} concentration needed for 50% of maximal force generation was significantly lower (i.e., higher pCa_{50}) for fibers from EDS patients with TNX deficiency vs. control fibers. Values are means ± SE.

deficient patients (Fig. 5*D*, *left*), resulting in significantly increased pCa_{50} values (Fig. 5*D*, *right*). Thus muscle fibers from patients with TNX deficiency display a significantly elevated calcium sensitivity, resulting in higher force generation at submaximal Ca^{2+} levels.

DISCUSSION

This study revealed that passive tension of sarcomeres from TNX-deficient EDS patients is markedly increased. The increased passive tension is caused by changes in the properties of the giant elastic sarcomeric protein titin that might be attributable to phosphorylation of titin's spring region. Whereas the active tension of sarcomeres at maximal activation level is similar between EDS patients with TNX deficiency and controls, tension at submaximal activation level is increased because of increased calcium sensitivity. Increased calcium sensitivity might be explained by the stiffer titin in the patients, which reduces myofilament lattice spacing, as low-angle X-ray diffraction experiments revealed. Thus, in response to the increased compliance of the *extra*cellular matrix in muscle of TNX-deficient EDS patients, profound *intra*cellular changes take place in the sarcomeric myofilaments.

Manifest Increase of Sarcomeric Passive Tension in EDS Patients with TNX Deficiency

TNX is abundantly expressed in the extracellular matrix of tendon and skeletal muscle (23), where it is involved in collagen deposition and maturation and linking collagen fibrils (6). A reduction in the density of collagen fibrils in the ECM, presumably attributable to impaired collagen deposition and network formation as a result of TNX deficiency, has been suggested to underlie increased compliance of connective tissues within and between the muscles and in the myotendinous pathways of TNX-deficient EDS patients (21, 38). Recent work on a TNX knockout mouse model suggested that the ECM abnormalities induce muscle weakness by impairing myofascial force transmission (17) (i.e., force transmission from muscle fibers onto the connective tissue within muscle and between adjacent muscles and fascia). Increased ECM compliance is thus likely to cause muscle weakness in EDS patients.

It is now well recognized that the extracellular matrix is an extremely dynamic complex of molecules that interacts through trans-sarcolemmal proteins with cytoskeletal elements within muscle fibers, such as the sarcomeres, to maintain skeletal muscle integrity and to transmit forces (19). Thus changes in the extracellular matrix might affect sarcomeric properties (37, 42).

To study sarcomere properties in TNX-deficient EDS patients, we isolated and skinned muscle fibers and measured both passive and active forces. A striking finding of the present study was the marked increase of passive tension of sarcomeres from EDS patients with TNX deficiency (Fig. 1*A*). Our experiments revealed that the high passive tension was not attributable to residual cross-bridge binding (Fig. 1, *B* and *C*) but was titin based.

Titin is a giant protein (~3–4 MDa) and constitutes the third filament of the sarcomere, after the thick and thin filaments (see Fig. 3*C* for a schematic representation) (11). Titin's NH_2 terminus is anchored in the Z-disc, and its COOH terminus extends to the M-band region of the sarcomere. The majority of titin's I-band region is extensible and functions as a molecular spring. This spring maintains the precise structural arrangement of thick and thin filaments (15) and gives rise to the passive tension of stretched sarcomeres (10). Titin's spring region in skeletal muscle is comprised of serially linked immunoglobulin (Ig)-like domains that make up the so-called tandem Ig segments and a segment rich in proline-glutamate-valine-lysine (PEVK) residues (35). Titin is encoded by a single gene that in humans contains 363 exons (2); alternative splicing leads to isoforms with distinct spring compositions (2). This makes titin an adjustable molecular spring, with mechanical properties that can be tuned according to the mechanical demands placed on muscle (27). To study whether the increased passive stiffness of EDS sarcomeres was caused by alternative splicing of the titin gene (rendering molecules with a shorter, and thus stiffer, PEVK spring region) we performed titin exon composition studies. However, these studies revealed no difference in exon composition, suggesting no difference in titin isoform composition between both groups (Fig. 3*C*). These findings were confirmed by Western blot studies showing no difference in the size of the PEVK region of titin (Fig. 3*D*).

Another pathway for adjusting titin's stiffness, in addition to alternative splicing, is posttranslational modification (22). Recent studies showed that titin's PEVK region contains two protein kinase C-α phosphorylation sites, one at S11878 (S26 in PEVK region) and one at S12022 (S170) (14), with evidence suggesting that hyperphosphorylation of S26 induces a large increase in passive stiffness (1, 14) and contributes to ventricular stiffening in diastolic dysfunction (16). Therefore, we recently developed novel phospho-specific antibodies to these two PEVK sites, and validation of these new antibodies was performed using recombinant protein subunits in which S26 and S170 were mutated. The antibodies were shown to be specific to the phospho-S26 or phospho-S170 (16). As shown in Fig. 4, our Western blotting studies revealed marked *hyper*phosporylation of S26 in the PEVK region of EDS patients with TNX deficiency. We propose that this hyperphosphorylation significantly contributes to the high passive stiffness of muscle fibers from TNX-deficient EDS patients. To test this proposition, future studies should investigate whether dephosphorylation of titin corrects the high passive stiffness. However, the large increase in passive stiffness in TNX-deficient muscle fibers (Fig. 1) is surprising and requires further study, including whether in addition to hyperphosphorylation of S26 in the PEVK region other mechanisms contribute as well.

The changes in passive tension in sarcomeres from EDS patients with TNX deficiency was not accompanied by changes in the maximum active tension at supramaximal calcium levels (pCa 4.5). These findings suggest that the mild muscle weakness observed in the studied patients (for details on in vivo muscle function, see Table 1) is not caused by impaired maximal sarcomere contractility. An interesting finding was that the tension cost was reduced (Fig. 2*D*), indicating that for a similar level of force production less ATP is consumed by sarcomeres from TNX-deficient EDS patients. This could be explained by a change in the cross-bridge cycle kinetics and a slower detachment rate of cross bridges from actin, prolonging the average duration of force generation by the cross bridge. Considering that muscle fibers from EDS patients need a higher level of active force to compensate for overall muscle

weakness, we speculate that this increased economy of contraction will help prevent the development of muscle fatigue by moderating ATP consumption.

Increased Titin-Based Stiffness: Effect on Muscle Contractility at Submaximal Activation?

The markedly higher titin-based passive stiffness in sarcomeres from EDS patients with TNX deficiency is likely to contribute to the increased calcium sensitivity of force generation that was observed (Fig. 5*D*). Several recent lines of evidence indicate that the lateral separation of thick and thin filaments within the sarcomere (i.e., myofilament lattice spacing) is regulated by titin as a lattice stabilizer via its passive force (5, 7, 18). Titin binds to the thin filament in and near the Z-disk (see Fig. 3*C*). Therefore, titin runs obliquely (not in parallel) to the thin and thick filaments, resulting in the production of radial forces as well as longitudinal forces in the lattice; radial forces pull the thin filament closer to the thick filament. This increases the likelihood of myosin attaching to the thin filament, thereby elevating the calcium sensitivity of force generation (5, 7, 18). Indeed, using X-ray diffraction we found that, in line with the increased passive tension, lattice spacing is reduced in sarcomeres from EDS patients with TNX deficiency (Fig. 5, *A* and *B*). Thus the stiffer titin molecules in EDS patients with TNX deficiency might contribute to the significantly enhanced calcium sensitivity of force generation by reducing myofilament lattice spacing. The Ca^{2+} sensitivity of force generation is an important determinant of muscle function, because in vivo skeletal muscle functions typically at submaximal activation. The increase in the Ca^{2+} sensitivity of force generation in muscle fibers from TNX-deficient EDS patients indicates that muscle fibers from patients generate a higher relative force than control fibers for similar Ca^{2+} concentrations. These findings might contribute to the previous observation that upon submaximal stimulation of m. quadriceps TNX-deficient EDS patients developed higher relative forces, i.e., increased twitch/tetanus ratio, than control subjects (36).

Conclusion

The present study reveals a marked increase in sarcomeric passive tension in muscle fibers from TNX-deficient EDS patients. This increased passive tension is at least partially caused by changes in the elastic properties of the sarcomeric protein titin attributable to altered phosphorylation. This suggests that the elevated muscle sarcomeric stiffness in EDS patients with TNX deficiency constitutes an intracellular compensation for the increased compliance of the extracellular matrix. Such interplay between extracellular and intracellular mechanisms has also been shown to occur in heart tissue (41) and might be a general phenomenon in striated muscle. Thus we propose that the muscle weakness attributable to increased compliance of the *extra*cellular matrix in TNX-deficient EDS patients is partly compensated *intra*cellularly by increased stiffness of titin.

ACKNOWLEDGMENTS

We thank Prof. Lammens (Dept of Pathology, Radboud University Nijmegen Medical Centre) for his work on the muscle biopsies of TNX-deficient patients.

GRANTS

This work was funded by a VENI grant from the Dutch Organization for Scientific Research to CACO, National Institutes of Health Grant RO1 AR060697 to H. Granzier, a clinical fellowship from the Princess Beatrix Foundation to N. C. Voermans.

DISCLOSURES

No conflicts of interest, financial or otherwise, are declared by the authors.

AUTHOR CONTRIBUTIONS

Author contributions: C.A.O., B.G.V.E., and H.L.G. conception and design of research; C.A.O., B.D.H., and T.C.I. performed experiments; C.A.O., B.D.H., and T.C.I. analyzed data; C.A.O., N.C.V., B.D.H., T.C.I., G.J.M.S., B.G.V.E., and H.L.G. interpreted results of experiments; C.A.O., N.C.V., B.D.H., and T.C.I. prepared figures; C.A.O., N.C.V., B.D.H., T.C.I., G.J.M.S., B.G.V.E., and H.L.G. drafted manuscript; C.A.O., N.C.V., B.D.H., T.C.I., G.J.M.S., B.G.V.E., and H.L.G. approved final version of manuscript.

REFERENCES

1. **Anderson BR, Bogomolovas J, Labeit S, Granzier H.** The effects of PKCalpha phosphorylation on the extensibility of titin's PEVK element. *J Struct Biol* 170: 270–277, 2010.
2. **Bang ML, Centner T, Fornoff F, Geach AJ, Gotthardt M, McNabb M, Witt CC, Labeit D, Gregorio CC, Granzier H, Labeit S.** The complete gene sequence of titin, expression of an unusual ~700-kDa titin isoform, and its interaction with obscurin identify a novel Z-line to I-band linking system. *Circ Res* 89: 1065–1072, 2001.
3. **Beighton P, De Paepe A, Steinmann B, Tsipouras P, Wenstrup RJ.** Ehlers-Danlos syndromes: revised nosology, Villefranche, 1997. Ehlers-Danlos National Foundation (USA) and Ehlers-Danlos Support Group (UK). *Am J Med Genet* 77: 31–37, 1998.
4. **Burch GH, Gong Y, Liu W, Dettman RW, Curry CJ, Smith L, Miller WL, Bristow J.** Tenascin-X deficiency is associated with Ehlers-Danlos syndrome. *Nat Genet* 17: 104–108, 1997.
5. **Cazorla O, Wu Y, Irving TC, Granzier H.** Titin-based modulation of calcium sensitivity of active tension in mouse skinned cardiac myocytes. *Circ Res* 88: 1028–1035, 2001.
6. **Egging D, Vlijmen-Willems I, van Tongeren T, Schalkwijk J, Peeters A.** Wound healing in tenascin-X deficient mice suggests that tenascin-X is involved in matrix maturation rather than matrix deposition. *Connect Tissue Res* 48: 93–98, 2007.
7. **Fukuda N, Wu Y, Farman G, Irving TC, Granzier H.** Titin-based modulation of active tension and interfilament lattice spacing in skinned rat cardiac muscle. *Pflügers Arch* 449: 449–457, 2005.
8. **Fukuda N, Wu Y, Nair P, Granzier HL.** Phosphorylation of titin modulates passive stiffness of cardiac muscle in a titin isoform-dependent manner. *J Gen Physiol* 125: 257–271, 2005.
9. **Granzier H, Radke M, Royal J, Wu Y, Irving TC, Gotthardt M, Labeit S.** Functional genomics of chicken, mouse, and human titin supports splice diversity as an important mechanism for regulating biomechanics of striated muscle. *Am J Physiol Regul Integr Comp Physiol* 293: R557–R567, 2007.
10. **Granzier HL, Irving TC.** Passive tension in cardiac muscle: contribution of collagen, titin, microtubules, and intermediate filaments. *Biophys J* 68: 1027–1044, 1995.
11. **Granzier HL, Labeit S.** The giant protein titin: a major player in myocardial mechanics, signaling, and disease. *Circ Res* 94: 284–295, 2004.
12. **Granzier HL, Wang K.** Interplay between passive tension and strong and weak binding cross-bridges in insect indirect flight muscle. A functional dissection by gelsolin-mediated thin filament removal. *J Gen Physiol* 101: 235–270, 1993.
13. **Greer KA, McReynolds MR, Brooks HL, Hoying JB.** CARMA: A platform for analyzing microarray datasets that incorporate replicate measures. *BMC Bioinformatics* 7: 149, 2006.
14. **Hidalgo C, Hudson B, Bogomolovas J, Zhu Y, Anderson B, Greaser M, Labeit S, Granzier H.** PKC phosphorylation of titin's PEVK element: a novel and conserved pathway for modulating myocardial stiffness. *Circ Res* 105: 631–638, 17, 2009.
15. **Horowits R, Podolsky RJ.** The positional stability of thick filaments in activated skeletal muscle depends on sarcomere length: evidence for the role of titin filaments. *J Cell Biol* 105: 2217–2223, 1987.

16. **Hudson B, Hidalgo C, Saripalli C, Granzier H.** Hyperphosphorylation of mouse cardiac titin contributes to transverse aortic constriction-induced diastolic dysfunction. *Circ Res* 109: 858–866, 2011.
17. **Huijing PA, Voermans NC, Baan GC, Buse TE, van Engelen BG, de Haan A.** Muscle characteristics and altered myofascial force transmission in tenascin-X-deficient mice, a mouse model of Ehlers-Danlos syndrome. *J Appl Physiol* 109: 986–995, 2010.
18. **Irving T, Wu Y, Bekyarova T, Farman GP, Fukuda N, Granzier H.** Thick-filament strain and interfilament spacing in passive muscle: effect of titin-based passive tension. *Biophys J* 100: 1499–1508, 2011.
19. **Jenniskens GJ, Veerkamp JH, Van Kuppevelt TH.** Heparan sulfates in skeletal muscle development and physiology. *J Cell Physiol* 206: 283–294, 2006.
20. **Konhilas JP, Irving TC, de Tombe PP.** Length-dependent activation in three striated muscle types of the rat. *J Physiol* 544: 225–236, 2002.
21. **Lethias C, Carisey A, Comte J, Cluzel C, Exposito JY.** A model of tenascin-X integration within the collagenous network. *FEBS Lett* 580: 6281–6285, 2006.
22. **LeWinter MM, Granzier H.** Cardiac titin: a multifunctional giant. *Circulation* 121: 2137–2145, 2010.
23. **Matsumoto K, Saga Y, Ikemura T, Sakakura T, Chiquet-Ehrismann R.** The distribution of tenascin-X is distinct and often reciprocal to that of tenascin-C. *J Cell Biol* 125: 483–493, 1994.
24. **Ottenheijm CA, Granzier H.** Role of titin in skeletal muscle function and disease. *Adv Exp Med Biol* 682: 105–122, 2010.
25. **Ottenheijm CA, Hidalgo C, Rost K, Gotthardt M, Granzier H.** Altered contractility of skeletal muscle in mice deficient in titin's M-band region. *J Mol Biol* 393: 10–26, 2009.
26. **Ottenheijm CA, Hooijman P, Dechene ET, Stienen GJ, Beggs AH, Granzier H.** Altered myofilament function depresses force generation in patients with nebulin-based nemaline myopathy (NEM2). *J Struct Biol* 170: 334–343, 2010.
27. **Ottenheijm CA, Knottnerus AM, Buck D, Luo X, Greer K, Hoying A, Labeit S, Granzier H.** Tuning passive mechanics through differential splicing of titin during skeletal muscle development. *Biophys J* 97: 2277–2286, 2009.
28. **Ottenheijm CA, Lawlor MW, Stienen GJ, Granzier H, Beggs AH.** Changes in cross-bridge cycling underlie muscle weakness in patients with tropomyosin 3-based myopathy. *Hum Mol Genet* 20: 2015–2025, 2011.
29. **Ottenheijm CA, van Hees HW, Heunks LM, Granzier H.** Titin-based mechanosensing and signaling: role in diaphragm atrophy during unloading? *Am J Physiol Lung Cell Mol Physiol* 300: L161–L166, 2011.
30. **Ottenheijm CA, Witt CC, Stienen GJ, Labeit S, Beggs AH, Granzier H.** Thin filament length dysregulation contributes to muscle weakness in nemaline myopathy patients with nebulin deficiency. *Hum Mol Genet* 18: 2359–2369, 2009.
31. **Prado LG, Makarenko I, Andresen C, Kruger M, Opitz CA, Linke WA.** Isoform diversity of giant proteins in relation to passive and active contractile properties of rabbit skeletal muscles. *J Gen Physiol* 126: 461–480, 2005.
32. **Schalkwijk J, Zweers MC, Steijlen PM, Dean WB, Taylor G, van Vlijmen IM, van Haren B, Miller WL, Bristow J.** A recessive form of the Ehlers-Danlos syndrome caused by tenascin-X deficiency. *N Engl J Med* 345: 1167–1175, 2001.
33. **Stienen GJ, Kiers JL, Bottinelli R, Reggiani C.** Myofibrillar ATPase activity in skinned human skeletal muscle fibres: fibre type and temperature dependence. *J Physiol* 493: 299–307, 1996.
34. **Trombitas K, Greaser M, French G, Granzier H.** PEVK extension of human soleus muscle titin revealed by immunolabeling with the anti-titin antibody 9D10. *J Struct Biol* 122: 188–196, 1998.
35. **Trombitas K, Greaser M, Labeit S, Jin JP, Kellermayer M, Helmes M, Granzier H.** Titin extensibility in situ: entropic elasticity of permanently folded and permanently unfolded molecular segments. *J Cell Biol* 140: 853–859, 1998.
36. **Voermans NC, Altenburg TM, Hamel BC, de Haan A, van Engelen BG.** Reduced quantitative muscle function in tenascin-X deficient Ehlers-Danlos patients. *Neuromuscul Disord* 17: 597–602, 2007.
37. **Voermans NC, Bonnemann CG, Huijing PA, Hamel BC, Van Kuppevelt TH, de Haan A, Schalkwijk J, van Engelen BG, Jenniskens GJ.** Clinical and molecular overlap between myopathies and inherited connective tissue diseases. *Neuromuscul Disord* 18: 843–856, 2008.
38. **Voermans NC, van Alfen N, Pillen S, Lammens M, Schalkwijk J, Zwarts MJ, van Rooij IA, Hamel BC, van Engelen BG.** Neuromuscular involvement in various types of Ehlers-Danlos syndrome. *Ann Neurol* 65: 687–697, 2009.
39. **Wang SM, Greaser ML.** Immunocytochemical studies using a monoclonal antibody to bovine cardiac titin on intact and extracted myofibrils. *J Muscle Res Cell Motil* 6: 293–312, 1985.
40. **Warren CM, Krzesinski PR, Greaser ML.** Vertical agarose gel electrophoresis and electroblotting of high-molecular-weight proteins. *Electrophoresis* 24: 1695–1702, 2003.
41. **Wu Y, Peng J, Campbell KB, Labeit S, Granzier H.** Hypothyroidism leads to increased collagen-based stiffness and re-expression of large cardiac titin isoforms with high compliance. *J Mol Cell Cardiol* 42: 186–195, 2007.
42. **Wu Y, Peng J, Campbell KB, Labeit S, Granzier H.** Hypothyroidism leads to increased collagen-based stiffness and re-expression of large cardiac titin isoforms with high compliance. *J Mol Cell Cardiol* 42: 186–195, 2007.